

Rotation-free Online Handwritten Character Recognition Using Linear Recurrent Units

Zhe Ling, Sicheng Yu, and Danyu Yang^(✉)

College of Mathematics and Statistics, Chongqing University, China
202306021008@stu.cqu.edu.cn, 20201868@stu.cqu.edu.cn,
danyuyang@cqu.edu.cn

Abstract. Online handwritten character recognition leverages stroke order and dynamic features, which generally provide higher accuracy and robustness compared with offline recognition. However, in practical applications, rotational deformations can disrupt the spatial layout of strokes, substantially reducing recognition accuracy. Extracting rotation-invariant features therefore remains a challenging open problem. In this work, we employ the Sliding Window Path Signature (SW-PS) to capture local structural features of characters, and introduce the lightweight Linear Recurrent Units (LRU) as the classifier. The LRU combine the fast incremental processing capability of recurrent neural networks (RNN) with the efficient parallel training of state space models (SSM), while reliably modelling dynamic stroke characteristics. We conducted recognition experiments with random rotation angle up to $\pm 180^\circ$ on three subsets of the CASIA-OLHDB1.1 dataset: digits, English upper letters, and Chinese radicals. The accuracies achieved after ensemble learning were 99.62%, 96.67%, and 94.33%, respectively. Experimental results demonstrate that the proposed SW-PS+LRU framework consistently surpasses competing models in both convergence speed and test accuracy.

Keywords: Online Handwritten Character Recognition · Sliding Window Path Signature · Linear Recurrent Unit.

1 Introduction

With the widespread adoption of smart terminals, Online Handwritten Character Recognition (OLHCR) now plays a key role in applications ranging from office automation to education. By directly capturing temporal stroke trajectories, OLHCR demonstrates superior discriminative capabilities compared to offline methods [1,2]. In many writing systems, characters are composed of semantic substructures—such as Chinese radicals—that play a central role in their recognition. Accurately recognizing these components not only boosts overall recognition accuracy but also facilitates downstream tasks like structural decomposition and character retrieval [3,4,5]. However, real-world factors like writing posture and device orientation frequently induce rotational deformations. Such deformations significantly alter stroke spatial layouts, causing confusion

among structurally similar classes [6]. This challenge is particularly pronounced in rotation-sensitive models, which suffer from severe performance degradation due to the high structural similarity of rotated characters.

While the path signature captures the geometry of a path [7], its global application is hindered by its high dimensionality and insensitivity to local changes [8]. To address these limitations, we adopt the Sliding Window Path Signature (SW-PS) method [9]. By segmenting the trajectory into chronological windows and computing the fixed-order signature for each, SW-PS effectively captures local dynamics while maintaining a manageable feature dimension. This approach balances global structure with local details, significantly enhancing robustness to rotational perturbations during training and inference.

In recent years, State Space Models (SSM) [10] have performed exceptionally well in long sequence modeling, capable of handling sequences with linear computational complexity and effectively capturing global dependencies. Inspired by the design of state space models, the Linear Recurrent Unit (LRU) proposed by the DeepMind team [11] improves the stability and modeling capabilities of traditional RNNs [12] in long sequence tasks through a series of optimizations such as complex diagonalization and linear recursion. The LRU's architecture retains high-accuracy modeling of temporal stroke patterns while enabling parallel training.

We conducted experiments on three subsets of the CASIA-OLHWDB1.1 dataset [1]: digits, English upper letters, and Chinese radicals. The proposed SW-PS+LRU framework consistently converged rapidly during training and achieved high test accuracy across all rotated subsets. The datasets and our code are publicly available. In contrast, when trained with the same procedure, classical CNN frameworks such as the ResNet series [39] fail to converge on randomly rotated datasets.

2 Related Works

The handwritten character recognition process can usually be divided into three main stages: data preprocessing, feature extraction and classification. Early dynamic time warping (DTW) [13] and principal component analysis (PCA) [14] can align and partially correct stroke trajectories. However, DTW remains vulnerable to temporal misalignment and doesn't provide any rotation normalization. While PCA can be effective for correcting rotated characters, it sometimes rotates the same character to different angles, making it harder to recognize [15]. Path signature features (PSF) [7] characterize the global trajectory structure through iterative integration, which can improve the local detail representation by increasing the truncation order. However, excessively high orders will cause the feature dimension to increase sharply. To address this, Yang and Jin [8] proposed a dyadic partition approach, in which the trajectory is recursively and evenly divided into 2^n segments at hierarchical level n , and path signature features are computed for each segment. In the classification stage, early approaches such as modified quadratic discriminant func-

tions (MQDF) [1] and discriminative learning quadratic discriminant functions (DLQDF) [16] achieved high recognition accuracy and stability, but had limited adaptability for handling complex spatial rotations and incurred high computational costs. With the successful application of deep convolutional neural networks (CNN) in image recognition, handwritten character recognition began to shift towards an end-to-end visual framework. Typical examples include CNN-Fujitsu [17] and multi-column deep neural networks (MCDNN) [18], which significantly outperformed traditional classifiers in terms of accuracy. Models such as DirectMap+ConvNet [19] effectively integrate hand-crafted geometric features with convolutional networks. The model in [20] further strengthens rotational robustness through a two-stage “rectify-then-recognize” procedure.

In addition to static image features, online handwriting trajectories incorporate the dynamic writing process, making time series modeling possible for handwriting recognition tasks. Recurrent neural networks (RNNs) [21], such as long short term memory networks (LSTM) [22] and gated recurrent units (GRU) [23], can capture sequence dependencies, but LSTM and GRU are serially dependent, difficult to parallelize and scale, and struggle with long sequences [10]. Transformers, the prevailing architecture for large language models, are highly effective but incur quadratic computational cost, making long-sequence modelling prohibitively expensive. On the other hand, State Space Models (SSM) [10] propagate information over time via parallel computation, enabling long-sequence modeling with linear complexity. State space model variants, such as LRU [11] and S5 [25], leverage simplified linear recurrence to effectively capture long-range dependencies. Neural Controlled Differential Equations (NCDE) [26] and Log Neural Controlled Differential Equations (Log-NCDE) [27] provide continuous-time representations for time series, but their reliance on numerical differential equation solvers results in high computational overhead, which limits their application.

In rotation-free online handwritten character recognition, the principal performance bottleneck arises from rotation-induced structural confusion. Our results show that SSMs achieve strong performance and are highly competitive for online character recognition.

3 Methods

3.1 Trajectory Preprocessing

Based on [28,29,30], our data preprocessing pipeline consists Removing Redundant Points, Penspeed Normalization, Character Rotation, Data Augmentation and Hanging Normalization. The workflow is shown in Fig. 1.

To preserve the temporal information of handwriting, we add an ink dimension [31] ink_i , where ink_i represents the writing order index. The input sequence is defined as $S = [(x_i, y_i, ink_i, p_i)]_{i=1}^l$, where (x_i, y_i) are coordinates and ink_i is the writing order index. The pen state p_i is a vector representing *pen-down* (0, 1), *continuous* (0, 0), or *pen-up* (1, 0) states.

To capture local dynamics, we compute first-order ($\Delta x, \Delta y$) and second-order ($\Delta^2 x, \Delta^2 y$) differences, representing velocity and acceleration. These differential features are linearly normalized to $(-1, 1)$ to eliminate scale bias. The final feature vector at each time step comprises $[x_i, y_i, \text{ink}_i, p_i, \Delta x_i, \Delta y_i, \Delta^2 x_i, \Delta^2 y_i]$. Trajectories are truncated or padded to a uniform length before the path signature extraction.



Fig. 1. Data preprocessing workflow.

Character Rotation Each handwritten sample is first rotated by a random angle α around the origin. The rotation transformation is defined as:

$$[x', y'] = [x, y] \begin{bmatrix} \cos \alpha & -\sin \alpha \\ \sin \alpha & \cos \alpha \end{bmatrix}$$

where $\alpha \in [0, 2\pi]$ represents the rotation angle.

Data Augmentation We enhance the dataset's diversity through data augmentation, using affine transformations and elastic distortions [32]. First, random scaling and translation are applied:

$$[x', y'] = [x, y] \begin{bmatrix} 1 + \delta_x & 0 \\ 0 & 1 + \delta_y \end{bmatrix} + [\delta_{t_x}, \delta_{t_y}]$$

where (δ_x, δ_y) represent random scaling factors affecting the aspect ratio, and $(\delta_{t_x}, \delta_{t_y})$ are small translation jitters. Additionally, an elastic distortion is introduced:

$$x'' = x' + \epsilon \sin(2\pi y'), \quad y'' = y' + \epsilon \sin(2\pi x')$$

Here, ϵ controls the deformation strength. By enriching the spatial configuration of handwritten strokes, the augmented dataset better represents various natural writing variations encountered in practice.

Hanging Normalization To achieve a rotation-free representation and mitigate writing style differences, we employ the hanging normalization method [33]. Hanging normalization assumes that the relative positions of two keypoints are stable. By aligning two keypoints to a fixed vertical direction, rotational compensation can be performed on characters before feature extraction. For the two keypoints, possible choices are the start point and center point (SC), the start point and end point (SE), and the average start point and average end point of all strokes (ASE). Previous study [8] has shown that SC achieves the most stable and reliable alignment. Therefore, we adopt the SC mode and briefly describe its formula.

Given an online handwritten character with T time steps $P = \{(x_t, y_t)\}_{t=1}^T$, we denote the starting point S and the center point C as:

$$S = (x_1, y_1), \quad C = (\bar{x}, \bar{y}) = \left(\frac{1}{T} \sum_{t=1}^T x_t, \frac{1}{T} \sum_{t=1}^T y_t \right)$$

The compensation angle θ for rotating the line connecting S and C to the vertical direction is calculated as:

$$\theta = \arctan \left(\frac{\bar{y} - y_1}{\bar{x} - x_1} \right) + \frac{\pi}{2}$$

Then, each point is rotated by $-\theta$ around S to obtain rotation-normalized coordinates.

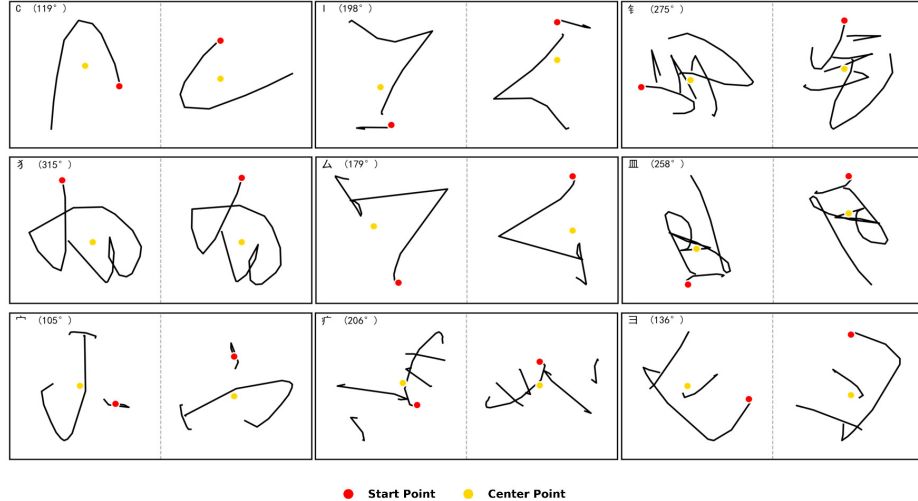


Fig. 2. Effect of Hanging Normalization in SC mode. The left side is "before", with the true label and rotation angle in the upper left corner. The right side is "after". The start red point is at the top and the center yellow point is at the bottom. Both are located on the same vertical line.

As shown in Fig. 2, the left side displays the online handwritten characters under random global rotation angles, while the right side shows the results after hanging normalization. It can be seen that the hanging normalization step effectively eliminates the directional differences caused by the rotation, ensuring that the stroke layout of the same character remains stable under different rotation angles, providing a more consistent input for the subsequent feature extraction and classification.

3.2 Sliding Window Path Signature

Path Signature The path signature traces back to Chen [34] in his work on geometric representation of paths, and was later systematically developed by Lyons in the Rough Path Theory [35]. It is obtained by computing iterated integrals on the coordinates of a path. This representation provides a top-down description of the geometry of the path: the first-order terms correspond to the total displacement along each coordinate axis; second-order terms are related to the signed area enclosed by the path together with the line segment from the end point to the starting point (as shown in Fig. 3).

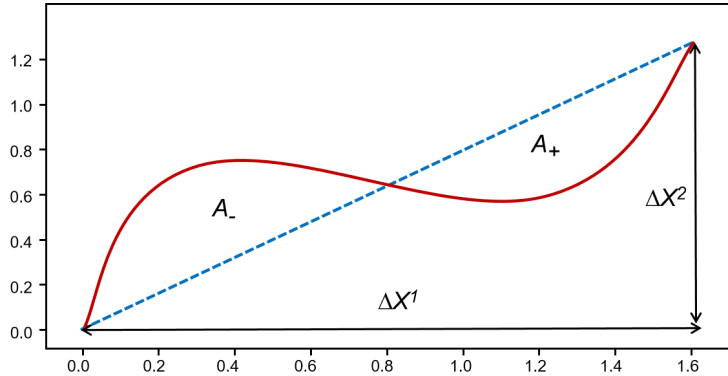


Fig. 3. Illustration of the step-2 truncated signature for a planar path (in red). The displacements ΔX^1 and ΔX^2 are the first level iterated integrals. The signed area $A_+ - A_-$ is a linear combination of second iterated integrals based on Green's theorem.

A discrete time series X can be linearly interpolated into a continuous trajectory:

$$X : [0, T] \rightarrow \mathbb{R}^d, \quad X_t = (X_t^1, X_t^2, \dots, X_t^d).$$

For a positive integer $k \geq 1$ and an index tuple (i_1, \dots, i_k) with $i_j \in \{1, 2, \dots, d\}$, the k -th iterated integral along X is defined as:

$$S_{0,T}^{i_1, \dots, i_k}(X) = \int_{0 < t_1 < \dots < t_k < T} dX_{t_1}^{i_1} \cdots dX_{t_k}^{i_k}.$$

The step- m truncated signature of a path X consists of all its iterated integrals upto level m , forming a finite sequence. It is defined as:

$$\text{Sig}_{0,T}^m(X) = \left(S_{0,T}^1(X), \dots, S_{0,T}^d(X), \dots, S_{0,T}^{i_1, \dots, i_m}(X), \dots, S_{0,T}^{d, \dots, d}(X) \right)$$

with dimension $\sum_{k=1}^m d^k$.

Sliding Window Path Signature Let the sequence X be (s_1, s_2, \dots, s_L) . We segment the sequence into overlapping windows where w is the window length and t is the step size [36]:

$$w_j = (s_{(j-1)t+1}, s_{(j-1)t+2}, \dots, s_{(j-1)t+w}), \quad j = 1, 2, \dots, K$$

Each window w_j is transformed using the m -th order signature mapping:

$$SW_j = \text{Sig}^m(w_j)$$

The total number of windows is given by:

$$K = \left\lfloor \frac{L-w}{t} \right\rfloor + 1$$

where $\lfloor \cdot \rfloor$ denotes the integer floor operation.

This windowed signature representation preserves sensitivity to local stroke deformations (e.g. elastic distortions) while maintaining the global series structure, making it well-suited for downstream sequence models.

3.3 Linear Recurrent Units (LRU)

In sequence modelling, traditional recurrent neural networks (RNNs) often encounter efficiency and stability issues during training, such as sequential processing constraints and vanishing or exploding gradients [22]. Linear Recurrent Neural Networks have emerged as a promising alternative, addressing the training efficiency issue by employing parallelizable linear recurrence. In particular, Linear Recurrent Units (LRU) are introduced in [10]:

$$h_t = Ah_{t-1} + Bx_t, \quad y_t = Ch_t + Dx_t,$$

where A, B, C, D are learnable parameters.

With careful initializations and parameterizations, LRU achieve strong performance on the Long Range Arena benchmark [11]. To achieve efficient parallelizable training, LRU utilize complex diagonal matrix A , allowing for a convolutional unrolling to compute the hidden representation $h_k = \sum_{j=0}^{k-1} A^j B x_{k-j}$ with $h_0 = B x_0$. Therefore, using the eigenvalue decomposition of a complex diagonalizable matrix A , we can write:

$$A = P \Lambda P^{-1}, \quad \Lambda = \text{diag}(\lambda_1, \dots, \lambda_{d_h})$$

Since real matrices that are complex-diagonalizable are dense [38], any n -by- n real matrix can be approximated by this decomposition. The diagonalization reduces matrix powers to element-wise operations $A^k = P \Lambda^k P^{-1}$, significantly boosting efficiency. The diagonal eigenvalues λ_i are parameterized in the complex exponential form:

$$\lambda_i = e^{-\nu_i + j\theta_i}, \quad \nu_i > 0$$

Here, θ_i captures periodic patterns, while ν_i controls the exponential decay rate. The constraint $\nu_i > 0$ ensures $|\lambda_i| < 1$, preventing the hidden state from exploding over long sequences and guaranteeing long-term stability [11].

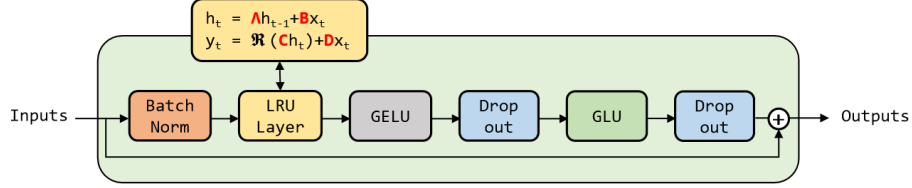


Fig. 4. The design of LRU Block. The Batch Norm mitigates covariate bias. The LRU Layer performs complex-valued linear recursion. Gaussian Error Linear Units (GELU) and Gated Linear Units (GLU) provide nonlinearities through smooth activation and learnable gating respectively. Dropout is applied between activations as a stochastic regularizer to mitigate overfitting and enhance generalization.

Overall Architecture of the Model After data preprocessing and SW-PS feature construction, we perform sequence classifications based on LRU. As shown in Fig. 5, our model consists three parts:

Linear Encoder Layer—Mapping the 90-dimensional SW-PS features of each window into a 256-dimensional hidden space.

Stacked LRU Blocks—The number of windows and the dimension of hidden layers remain constant in the stacked modules. As shown in Fig. 4, each block consists of three parts:

- (1) Linear recurrence. The input is batch normalized and then fed to a complex-valued recursive LRU layer $h_t = Ah_{t-1} + Bx_t$;
- (2) Non-linear gating. The the inherent linearity of the LRU is compensated through a composite gating path: GELU \rightarrow Dropout \rightarrow GLU \rightarrow Dropout;
- (3) Residual connection. Input is added to the output to facilitate gradient flow.

Output Layer—Features from all windows are reduced in dimension using Global Average Pooling, and the class probabilities are generated by the final dense layer.

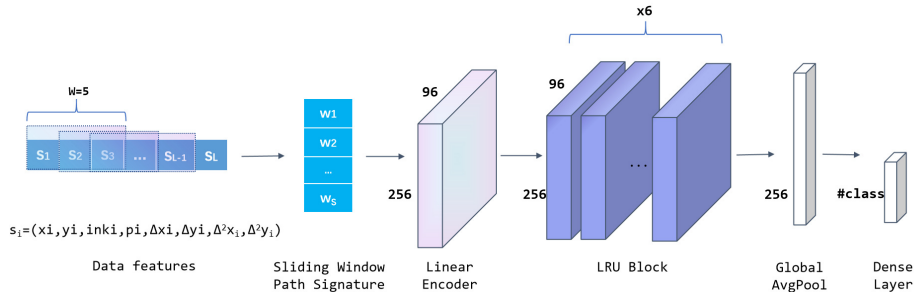


Fig. 5. Overall Architecture of the Model.

4 Experiments

4.1 Experimental Setups

Experiments were conducted on three subsets of the CASIA-OLHWDB1.1 dataset: Digits (10 classes), English Upper Letters (26 classes), and Chinese Radicals (52 classes). The Chinese radicals are shown in Fig. 6. Each class contains approximately 300 samples, split into 240 for training and 60 for testing. During model training, we first applied global random rotations to the characters. Furthermore, to simulate local variations in practice, we employed a composite augmentation strategy involving random affine scaling, translation, and elastic distortion. The local augmentation was applied exclusively during training to enrich structural diversity. In the testing phase, we generated 30 variations for each original sample by rotating it at 12° intervals, resulting in a test set 30 times larger than the original. Rotating samples at 12° intervals provides well-rounded test scenarios and avoids the randomness introduced by arbitrary rotation during testing.

We utilized the Adam optimizer with global gradient clipping to prevent gradient explosion. A stepwise learning rate schedule was employed with an initial rate of 10^{-3} , decaying by a factor of $\gamma = 0.5$ every $T_s = 4500$ steps, down to a minimum of 10^{-6} . This schedule effectively balances optimization stability and convergence speed. The objective function combines cross-entropy loss with L2 regularization, and a dropout rate of 0.3 was applied to mitigate overfitting.

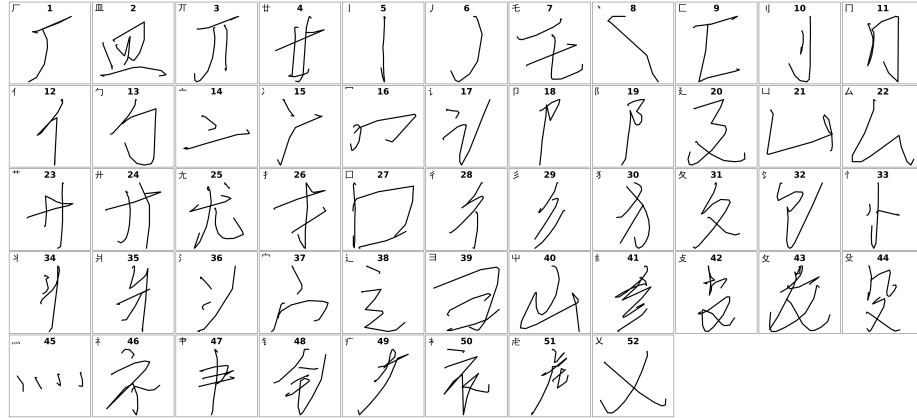


Fig. 6. Samples of 52 Chinese radicals.

4.2 Evaluation of SW-PS and Hanging Normalization

This section evaluates the impact of different window sizes, truncation degrees, and hanging normalization. Since the Chinese radical dataset presents a greater

classification challenge than other two datasets, we selected it for these experiments. Preliminary tests indicated that the stride had negligible impact. Hence, we fixed the stride to 1 for all cases.

Due to memory overflow encountered with degree-3 path signatures, we limited our comparison to degree-1 and degree-2 signatures, as shown in Table 1. Excessively large windows fail to capture local details, whereas a window size of 1 prevents path signatures from capturing nonlinear interactions between channels. Therefore, we evaluated window sizes of 2, 5, 10, 15 and 20 with LRU as the downstream model.

Table 1. Test accuracy with different sliding window size w , truncation degree m and hanging normalization on the Chinese radical dataset.

Test Accuracy (%)		Window size w				
		2	5	10	15	20
Truncation	1	No Hanging	88.89	89.36	86.86	85.75
	2	Normalization	90.01	90.51	89.06	88.23
Degree m	1	Hanging	92.85	93.21	93.08	92.78
	2	Normalization	92.92	93.37	93.26	93.24

As shown in Table 1, hanging normalization consistently improves accuracy by 3% to 4% across various hyperparameter combinations. Furthermore, degree-2 signatures generally outperform degree-1 signatures. The configuration using a window size of 5, truncation degree of 2, and hanging normalization achieved the highest recognition accuracy of 93.37%. Consequently, we adopt this configuration for all subsequent experiments.

4.3 Evaluation of different models

This section evaluates the performance of different downstream models. Among them, RFOLHCR is our reproduction of the model from [8]. We compare three models utilizing path signature features (LRU, S5, and RFOLHCR) against two models based on rough path theory (NCDE and Log-NCDE) [35]. NCDE and Log-NCDE are continuous-time models that rely on differential equation solvers and are therefore computationally intensive. Owing to memory constraints, NCDE and Log-NCDE do not employ path signature features, which, as our results demonstrate, leads to degraded performance.

Table 2. Results of different downstream models on three datasets.

Test Accuracy (%)	LRU	S5	NCDE	Log-NCDE	RFOLHCR
Digits	99.17	99.15	97.50	97.72	98.07
English Upper Letters	95.71	95.63	89.18	90.59	93.21
Chinese Radicals	93.37	93.19	84.69	85.14	88.47

Table 2 reports the average test accuracy over 10 random seeds (standard deviations are omitted as they are all within 0.5%). The LRU model consistently achieved the highest accuracy across all three datasets, outperforming the results reported in [8]. S5 and our reproduced RFOLHCR followed, while NCDE and Log-NCDE performed the worst. This indicates that path signature features effectively capture discriminative characteristics. Our reproduction of RFOLHCR did not achieve the accuracy reported in the original paper [8]. This discrepancy is likely due to differences in data preprocessing procedures and experimental settings, such as hyperparameters or random seeds. Additionally, we evaluated the ResNet [39] as a representative classical CNN-based computer vision model. The ResNet series fails to converge, resulting in poor performance, which we therefore did not report.

Table 3. Soft vs. Hard voting ensemble test accuracy (%).

Test Accuracy (%)		LRU	S5	NCDE	Log-NCDE	RFOLHCR
Digits	Soft	99.62	99.39	98.17	97.94	98.67
	Hard	99.61	99.37	98.00	97.83	98.83
English Upper Letters	Soft	96.67	96.21	91.08	92.31	94.68
	Hard	96.58	95.99	90.16	92.05	94.32
Chinese Radicals	Soft	94.33	93.89	87.24	87.60	89.99
	Hard	94.30	93.84	86.85	87.02	90.05

Table 3 shows the results of ensemble learning on models trained with 10 random seeds. We evaluated both soft voting and hard voting. Soft voting derives the final result by averaging the predicted probabilities, while hard voting makes the ensemble decision based on the majority count of the predicted labels. The results confirm that ensemble learning improves accuracy, with soft voting yielding an approximately 1% increase in test accuracy on the challenging Chinese radical dataset.

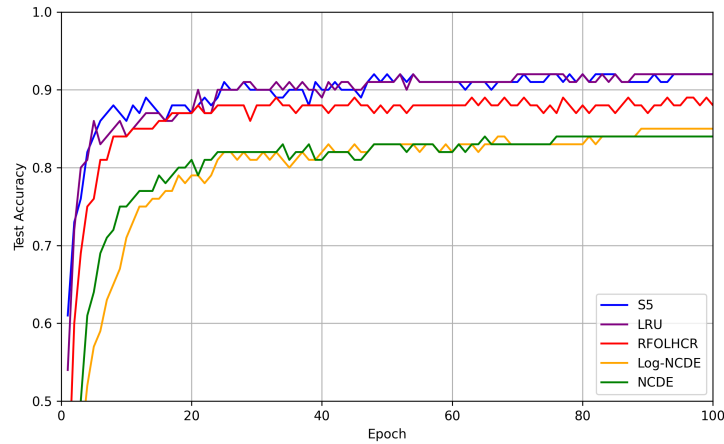


Fig. 7. Test accuracy on the Chinese Radical dataset (first 100 epochs).

We also analyzed the convergence speed of different models. As shown in Fig. 7, both LRU and S5 reached high accuracy within the first 20 epochs and continue to improve thereafter, demonstrating superior training efficiency compared with the other baselines.

Table 4. Impact of rotation angle ranges on the Chinese radical dataset.

Training Set	Testing Set	Test Accuracy (%)
Non-rotated	Non-rotated	94.63
Rotated within $\pm 15^\circ$	Rotated within $\pm 15^\circ$	94.48
Rotated within $\pm 45^\circ$	Rotated within $\pm 45^\circ$	93.54
Rotated within $\pm 180^\circ$	Rotated within $\pm 180^\circ$	93.25

Table 4 presents the results on the Chinese radical dataset under different rotation ranges. As the rotation range expands from $\pm 15^\circ$ to $\pm 180^\circ$, the accuracy declines slightly. Large-degree rotations alter key structural features, causing confusion between similar radicals. For instance, in Fig. 8, a “ γ ” rotated by 264° geometrically resembles “ $\dot{\gamma}$ ”, leading to misclassification. On the other hand, a “ $\dot{\gamma}$ ” rotated by 60° retains its structural features and is correctly differentiated from “ γ ”. These samples illustrate that large-degree rotations introduce considerable ambiguity, whereas our proposed pipeline preserves high recognition accuracy despite these challenges.

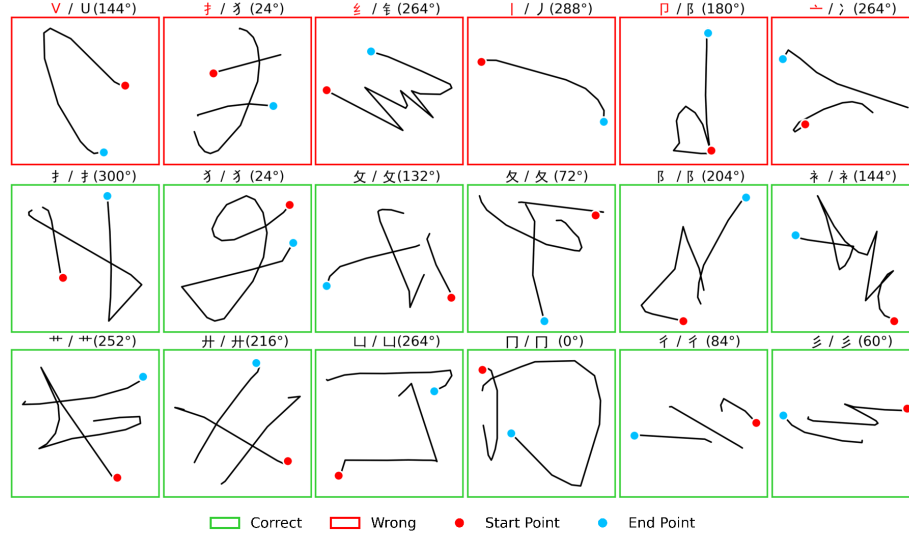


Fig. 8. Sample test results. The predicted class is in the top left, and the true label is in the top right, with the rotation angle indicated in brackets. The first row consists of samples that our method fails to recognise, while the second and third rows contain samples that are classified correctly.

Finally, Fig. 8 visualizes some of the test results. The first row displays some of the misclassified samples: a rotated “U” is mistaken for “V”, “ঁ” for “ং”, and “ঃ” for “ঁ”. These characters exhibit high structural similarities, making them difficult to distinguish even without rotation. In the second and third rows, our method correctly classifies the ambiguous characters, highlighting its discriminative capabilities. Some samples are difficult to discern, even for humans.

5 Conclusions

This paper proposes an OLHCR framework that integrates SW-PS features extraction with LRU-based classification. By leveraging path signature features and the sequence modeling capabilities of LRU, our model effectively balances local stroke variations with the global trajectory structure. As a result, our model achieves fast convergence and high test accuracy, whereas the classical ResNet series suffers from poor convergence and degraded performance under rotation. Future work could explore the application of our system to rotation-free Chinese characters recognition e.g. CASIA-OLHWBD1.1 or handwritten characters in other languages.

Acknowledgements.

DY gratefully acknowledges the support of the National Natural Science Foundation of China (Young Scholar Grant 12201081), Chongqing University (Starting Grant 02080011044104) and the Engineering and Physical Sciences Research Council (Programme Grant EP/S026347/1).

Data and Code Availability.

The data is publicly available at <https://doi.org/10.6084/m9.figshare.30759515>. Our code is available at https://github.com/ling17154/Character_Recognition.

References

1. Liu, C.: Online and offline handwritten Chinese character recognition: Benchmarking on new databases. *Pattern Recognit.* **46**(1), 155–162 (2013)
2. Yadav, P., Yadav, N.: Handwriting recognition system-a review. *Int. J. Comput. Appl.* **114**(19), 36–40 (2015)
3. Shi, D., Gunn, S.: Handwritten Chinese radical recognition using nonlinear active shape models. *IEEE Trans. Pattern Anal. Mach. Intell.* **25**(2), 277–280 (2003)
4. Zhang, J., Du, J.: Radical analysis network for learning hierarchies of Chinese characters. *Pattern Recognit.* **103**, 107305 (2020)
5. Daniels, P.: Writing systems. In: Aronoff, M., Rees-Miller, J. (eds.) *The Handbook of Linguistics*, 2nd edn, pp. 75–94. Wiley-Blackwell, Hoboken (2017)
6. Huang, S., Jin, L.: A novel approach for rotation free online handwritten Chinese character recognition. In: *Proceedings of the 10th International Conference on Document Analysis and Recognition*, pp. 1136–1140. IEEE, Barcelona (2009)

7. Graham, B.: Sparse arrays of signatures for online character recognition. arXiv preprint arXiv:1307.7291 (2013)
8. Yang, W., Jin, L.: Rotation-free online handwritten character recognition using dyadic path signature features, hanging normalization, and deep neural network. In: Proceedings of the 23rd International Conference on Pattern Recognition, pp. 4083–4088. IEEE, Cancun (2016)
9. Yang, W., Lyons, T.: Developing the path signature methodology and its application to landmark-based human action recognition. In: Crisan, D., Hambly, B., Zariphopoulou, T. (eds.) Stochastic Analysis, Filtering, and Stochastic Optimization, pp. 431–464. Springer, Cham (2022)
10. Gu, A., Goel, K.: Efficiently modeling long sequences with structured state spaces. In: International Conference on Learning Representations (2022)
11. Orvieto, A., Smith, S., Gu, A.: Resurrecting recurrent neural networks for long sequences. In: Proceedings of the 40th International Conference on Machine Learning, PMLR, vol. 202, pp. 26670–26698 (2023)
12. Elman, J.: Finding structure in time. *Cogn. Sci.* **14**(2), 179–211 (1990)
13. Rakthanmanon, T., Campana, B., Mueen, A.: Searching and mining trillions of time series subsequences under dynamic time warping. In: Proceedings of the 18th ACM SIGKDD International Conference on Knowledge Discovery and Data Mining, pp. 262–270. ACM, Beijing (2012)
14. Abdi, H., Williams, L.: Principal component analysis. *Wiley Interdiscip. Rev. Comput. Stat.* **2**(4), 433–459 (2010)
15. Simard, P., Steinkraus, D., Platt, J.: Best practices for convolutional neural networks applied to visual document analysis. In: Proceedings of the 7th International Conference on Document Analysis and Recognition, pp. 958–963. IEEE, Edinburgh (2003)
16. Kimura, F., Takashina, K., Tsuruoka, S., Miyake, Y.: Modified quadratic discriminant functions and the application to Chinese character recognition. *IEEE Trans. Pattern Anal. Mach. Intell.* **9**(1), 149–153 (1987)
17. Yin, F., Wang, Q., Zhang, X., Liu, C.: ICDAR 2013 Chinese handwriting recognition competition. In: Proceedings of the 12th International Conference on Document Analysis and Recognition, pp. 1464–1470. IEEE, Washington, DC (2013)
18. Cireşan, D., Meier, U.: Multi-column deep neural networks for offline handwritten Chinese character classification. In: Proceedings of the 2015 International Joint Conference on Neural Networks, pp. 1–6. IEEE, Killarney (2015)
19. Zhong, Z., Jin, L., Xie, Z.: High performance offline handwritten Chinese character recognition using GoogLeNet and directional feature maps. In: Proceedings of the 13th International Conference on Document Analysis and Recognition, pp. 846–850. IEEE, Tunis (2015)
20. Li, Z., Jin, L., Lai, S.: Rotation-free online handwritten Chinese character recognition using two-stage convolutional neural network. In: Proceedings of the 16th International Conference on Frontiers in Handwriting Recognition, pp. 205–210. IEEE, Niagara Falls (2018)
21. Zhang, X., Yin, F., Zhang, Y., Liu, C.: Drawing and recognizing Chinese characters with recurrent neural network. *IEEE Trans. Pattern Anal. Mach. Intell.* **40**(4), 849–862 (2018)
22. Hochreiter, S., Schmidhuber, J.: Long short-term memory. *Neural Comput.* **9**(8), 1735–1780 (1997)
23. Cho, K., van Merriënboer, B., Gulcehre, C.: Learning phrase representations using RNN encoder–decoder for statistical machine translation. In: Proceedings of the

2014 Conference on Empirical Methods in Natural Language Processing, pp. 1724–1734. ACL, Doha (2014)

24. Vaswani, A., Shazeer, N., Parmar, N., Uszkoreit, J.: Attention is all you need. In: Advances in Neural Information Processing Systems, vol. 30, pp. 5998–6008 (2017)
25. Smith, J.T.H., Warrington, A., Linderman, S.W.: Simplified state space layers for sequence modeling. In: International Conference on Learning Representations (2023)
26. Kidger, P., Morrill, J., Foster, J.: Neural controlled differential equations for irregular time series. In: Advances in Neural Information Processing Systems, vol. 33, pp. 6696–6707. Curran Associates, Red Hook (2020)
27. Walker, B., McLeod, A., Qin, T., Cheng, Y.: Log neural controlled differential equations: The Lie brackets make a difference. In: Proceedings of the 41st International Conference on Machine Learning, PMLR, vol. 235, pp. 49822–49844 (2024)
28. Pastor, M.: Writing speed normalization for online handwritten text recognition. In: Proceedings of the 8th International Conference on Document Analysis and Recognition, vol. 2, pp. 1131–1136. IEEE, Seoul (2005)
29. Xiao, W., Chen, S., Ma, Y.: Integrating path signature and pen-tip trajectory features for online handwriting Yi text recognition. *Herit. Sci.* **12**, 376 (2024)
30. He, T., Huo, Q.: A character-structure-guided approach to estimating possible orientations of a rotated isolated online handwritten Chinese character. In: Proceedings of the 10th International Conference on Document Analysis and Recognition, pp. 536–540. IEEE, Barcelona (2009)
31. Okamoto, M., Yamamoto, K.: On-line handwriting character recognition method with directional features and direction-change features. In: Proceedings of the 4th International Conference on Document Analysis and Recognition, vol. 2, pp. 926–930. IEEE, Ulm (1997)
32. Simard, P.Y., Steinkraus, D., Platt, J.C.: Best practices for convolutional neural networks applied to visual document analysis. In: Proceedings of the 7th International Conference on Document Analysis and Recognition, vol. 1, pp. 958–963. IEEE Computer Society, Edinburgh (2003)
33. Du, J., Huo, Q., Chen, K.: Designing compact classifiers for rotation-free recognition of large vocabulary online handwritten Chinese characters. In: Proceedings of the 2012 IEEE International Conference on Acoustics, Speech and Signal Processing, pp. 1721–1724. IEEE, Kyoto (2012)
34. Chen, K.: Integration of paths-a faithful representation of paths by noncommutative formal power series. *Trans. Am. Math. Soc.* **89**(2), 395–407 (1958)
35. Lyons, T.: Differential equations driven by rough signals. *Rev. Mat. Iberoam.* **14**(2), 215–310 (1998)
36. Chevyrev, I., Kormilitzin, A.: A primer on the signature method in machine learning. In: Kormilitzin, A., et al. (eds.) *Signature Methods in Finance: An Introduction with Computational Applications*, pp. 3–64. World Scientific (2025)
37. Yue, Z., Wang, Y.: Linear recurrent units for sequential recommendation. In: Proceedings of the 17th ACM International Conference on Web Search and Data Mining, pp. 930–938. ACM, Merida (2024)
38. Horn, R., Johnson, C.: *Matrix Analysis*, 2nd edn. Cambridge University Press, Cambridge (2013)
39. He, K., Zhang, X., Ren, S., Sun, J.: Deep residual learning for image recognition. In: Proceedings of the IEEE Conference on Computer Vision and Pattern Recognition, pp. 770–778. IEEE, Las Vegas (2016)